THE JOURNAL OF PHYSICAL CHEMISTRY Letters

Letter

pubs.acs.org/JPCL

High Contrast Visualization of Cell–Hydrogel Contact by Advanced Interferometric Optical Microscopy

Takahisa Matsuzaki,[†] Gen Sazaki,[‡] Masami Suganuma,[§] Tatsuro Watanabe,[§] Takashi Yamazaki,[†] Motomu Tanaka,[∥,⊥] Seiichiro Nakabayashi,[†] and Hiroshi Y. Yoshikawa*[,†]

[†]Department of Chemistry, Saitama University, Sakura-ku, Saitama, 338-8570, Japan

[‡]The Institute of Low Temperature Science, Hokkaido University, N19-W8, Sapporo 060-0819, Japan

[§]Research Institute for Clinical Oncology, Saitama Cancer Center, Kitaadachi-gun, Saitama 362-0806, Japan

[∥]Physical Chemistry of Biosystems, Institute of Physical Chemistry, University of Heidelberg, D69120 Heidelberg, Germany

[⊥]Institute for Integrated Cell-Material Sciences (WPI iCeMS), Kyoto University, 606-8501, Kyoto, Japan

Supporting Information

ABSTRACT: Hydrogels with tunable elasticity has been widely used as micromechanical environment models for cells. However, the imaging of physical contacts between cells and hydrogels with a nanometer resolution along the optical axis remain challenging because of low reflectivity at hydrogel-liquid interface. In this work, we have developed an advanced interferometric optical microscopy for the high contrast visualization of cell-hydrogel contact. Here, reflection interference contrast microscopy (RICM) was modified with a confocal unit, high throughput optics and coherent monochromatic light sources to enhance interferometric signals from cell-hydrogel contact zones. The advanced interferometry clearly visualized physical contacts between cells and hydrogels, and thus enabled the quantitative evaluation of the area of cell-hydrogel adhesion.

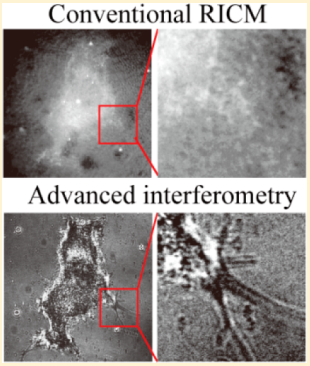

SECTION: Biophysical Chemistry and Biomolecules

Recently, a number of studies revealed that cells sensitively response to mechanical properties of their environments via adhesion sites (the so-called mechano-response).[1,2] To study such cell mechano-response, hydrogels with tunable elasticity has been widely used as micromechanical environment models for cells. However, the imaging of physical contacts between cells and hydrogels with a nanometer resolution along the optical axis remain challenging. So far, total internal reflection fluorescence (TIRF) microscopy has been widely used to visualize cell adhesion molecules near substrate. However, height resolution of TIRF (100–200 nm)[3] is not sufficient to identify the physical contact between cells and substrate. Alternatively, the leading technique for visualizing cell–substrate contacts is reflection interference contrast microscopy (RICM), which detects interference of linearly polarized light reflected at cell–liquid (i.e., cell membrane–liquid) and substrate–liquid interfaces.[4−9] If solid substrate (e.g., glass) is used, RICM is a powerful label-free technique to measure the thickness of water reservoir between cells and substrates with a resolution of ∼2 nm,[9] which is much finer than surface-sensitive fluorescence techniques such as TIRF microscopy. However, in the case of hydrogel, the contrast of RICM images becomes very poor because of the following two reasons. First, the refractive index of hydrogels is very close to that of water, which results in low reflectivity at hydrogel–liquid interfaces. Second, the thickness of gels used for such studies is typically several micrometers or beyond, and thus the contrast of interferometric patterns become poor. Although RICM combined with a confocal system was proposed to visualize the cells adherent to glass substrates modified with a carbon monolayer or thin polymer layers,[10,11] RICM has not been applied to soft, thick hydrogels to evaluate cell mechano-response.

In this account, we have developed an interferometric optical microscopy for the high contrast visualization of cell-hydrogel contact. As schematically illustrated in Figure 1a, conventional RICM setup utilizes the antiflex method:[5] cross polarizers combined with an objective lens equipped with a quarter-wave plate (Antiflex EC Plan-Neofluar, 63 x, Numerical aperture = 1.25, Oil Ph3, Zeiss, Gottingen, Germany). A mercury lump with a monochromatic filter (typically λ = 546 nm) has been widely used as a light source. To enhance the contrast of interference images obtained from cell-hydrogel contact, we modified the RICM setup by the three points enlisted below (Figure 1b). (1) A confocal unit (FV300, Olympus, Tokyo, Japan) was attached to an inverted microscope (IX70,

Received: November 15, 2013
Accepted: December 19, 2013
Published: December 19, 2013

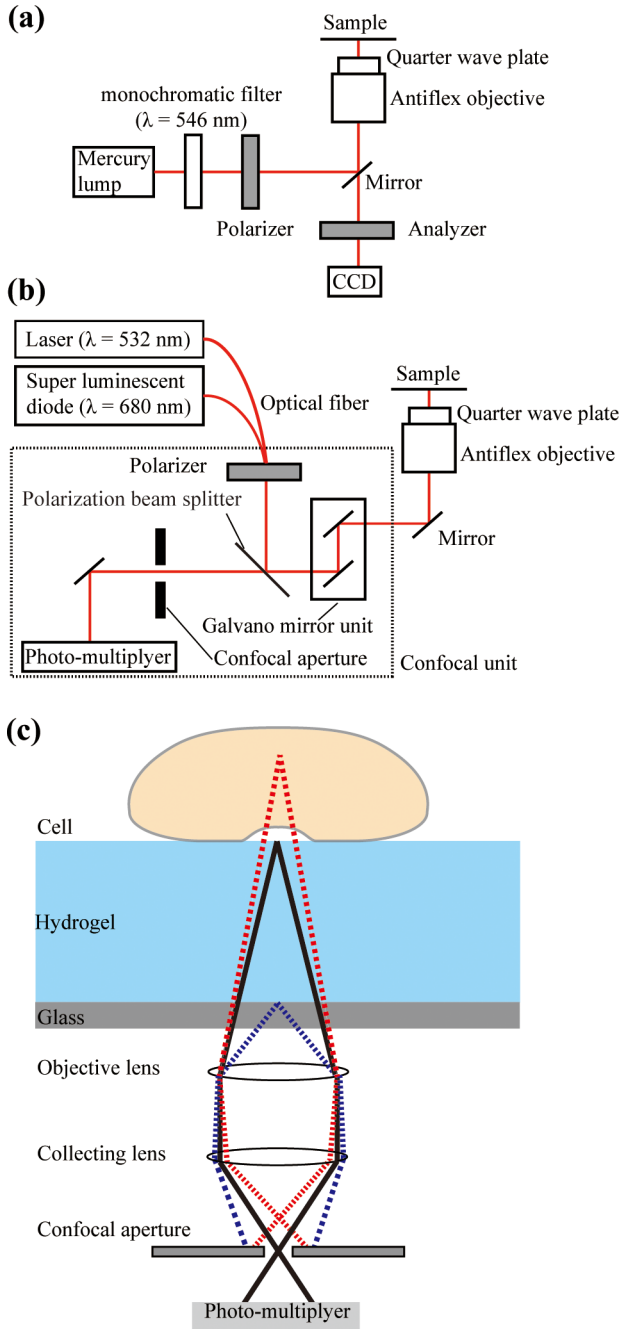

Figure 1. Schematic illustration of experimental setup of (a) a conventional RICM and (b) the interferometric microscopy developed in this study. (c) A confocal aperture reduces untargeted stray light originating from glass (blue dashed line), cell cytoplasm, and organelle (red dashed line).

Olympus, Tokyo, Japan). A confocal aperture in the unit can significantly reduce stray light originating from outside of cell-hydrogel contact zones, e.g., reflection and scattering from glass, gels, cell cytoplasm, and organelle (Figure 1c). (2) High-throughput optics mentioned in the following was adopted to increase intensity and hence to further improve the signal-to-noise ratio. First, a polarization beam splitter (PBS, custom-ordered, Olympus Tokyo, Japan) that reflects s-polarized light and transmits p-polarized light over 95% at the light wavelength was used. The use of the PBS instead of a half mirror and an analyzer can drastically increase light intensity of both illumination and detection in the antiflex setup, while a half mirror splits light at the both sides. Second, a polarizer made of aligned silver nanoparticles (colorPol VISIR CWO2, CODIXX AG, Barleben, Germany) was used, because it can enhance the signals by an order of magnitude than the polarizer based on polymer films.[12] (3) As a light source, a diode-pumped solid state laser (λ = 532 nm, 300 mW, SAPPHIRE 532-300-CW-CDPH, Coherent Inc., Santa Clara, USA) or a super luminescent diode (SLD) (λ = 680 nm, 5mW, coherent length ~10 μm, ASLD68-050-B-FA, Amonics, Hong-Kong, China) was used. The use of such an intense monochromatic light source instead of halogen lamps should result in clearer interference patterns. In addition, since the coherent length of the solid-state laser and SLD is generally shorter than a gas laser like a He−Ne laser,[14] the use of light sources with such "moderate" coherence is expected to reduce untargeted interference signals except for cell-hydrogel contact zones.[13,14] In fact, Sazaki et al. demonstrated the high-contrast visualization of ice and protein crystal surfaces at atomic resolution by using a SLD as a light source for scanning confocal microscopy combined with differential interference contrast microscopy.[15] As gel substrate, polyacrylamide (PAAm) gels with a thickness of 6−7 μm were prepared on a glass slip according to the previously reported protocols.[16,17] Young's moduli (E) of PAAm gels were determined by the nanoindentation measurement using an atomic force microscope (MFP-3D, Asylum research, Santa Barbara, USA) with a silicon-nitride cantilever with a pyramidal tip with a spring constant of k = 0.02 N/m (TR400-PSA, Olympus, Tokyo, Japan).

Figure 2a−c shows interference images of a polystyrene latex bead with 100 μm diameter (Φ) (64220-15, Polyscience, Pennsylvania, USA) on a PAAm gel (E = 13.2 ± 0.5 kPa) taken by a conventional RICM set up and by our interferometric microscope system, respectively. The setup developed in this study provided much clearer interference patterns than those by a conventional RICM system. It should be also noted that both light sources, laser and SLD, show clear Newton's ring-like fringes without untargeted interference such as speckle, which is often formed in the case of a He−Ne laser as a light source.[13,14] From the intensity profile (Figure 2e), the height profile of a bead can be reconstructed (Figure 2d) according to eq 1:[8,9]

$$\frac{2I - (I_{max} + I_{min})}{-(I_{max} - I_{min})} = \frac{\sin y}{y} \cos\left\{\frac{4\pi n}{\lambda}\left[h\left(1 - \sin^2\left(\frac{\alpha}{2}\right)\right)\right]\right\} \quad (1)$$

Here, I is measured intensity. I_{max} and I_{min} are maximum and minimum intensity. λ is wavelength of light, h is the separation between substrate and sample, and n is the refractive index of the medium (~1.333). y represents $2\pi n \sin^2(\alpha/2)/\lambda$, where α is a half angle of the cone illumination (55°). The height profile of a bead reconstructed from interference signals by our system is in good agreement with the predicted height profile of a bead (Φ = 100 μm) up to 2 μm apart from the surface. The obtained results clearly demonstrate that our interferometry system is advantageous over conventional RICM, as it can provide clearer interferometric patterns to calculate the height profile of objects on hydrogels.

In the next step, we visualized cells adherent on hydrogels using a conventional RICM setup and our interferometric microscope. Figure 3a shows a bright field image of a mouse

dx.doi.org/10.1021/jz402463u | J. Phys. Chem. Lett. 2014, 5, 253−257

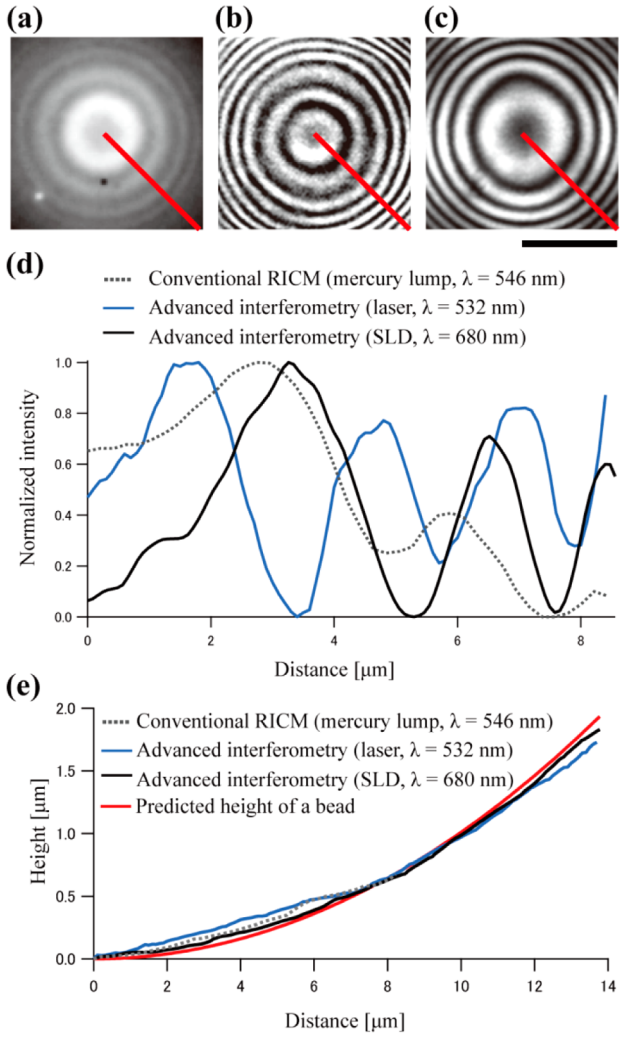

Figure 2. Interference images of polystyrene latex bead 100 μm in diameter on PAAm gels (E = 13.2 ± 0.5 kPa) taken by (a) conventional RICM and interferometric microscopy developed in this study with a light source of (b) laser or (c) SLD. Scale bars: 10 μm. Size of confocal aperture is 60 μm. (d) Intensity profiles along the red lines in panels a–c and (e) reconstructed and predicted height profiles of a bead.

metastatic melanoma cell (B16-F10) on a PAAm gel (E = 13.2 ± 0.5 kPa) functionalized with fibronectin (33010-018, Life Technologies Japan, Tokyo, Japan). Cells were cultured for 3 h in Leibovitz's L-15 medium (11415-064, Invitrogen, Life Technologies Japan, Tokyo, Japan) without serum and then fixed with a 3.7 w/v % DPBS-formaldehyde solution. With a conventional RICM, the cell came out brighter than its surrounding region, indicating that scattered light from outside of a focal plane (e.g., cell cytoplasm) obscured interference signals (Figure 3b). On the other hand, our interferometric microscope yielded a black cell body in sharp contrast against the bright surrounding region (Figure 3c–e). To assess influence of stray light on the image contrast of our interferometry, cell images were taken with different confocal aperture diameters. The image contrast became higher by reducing the aperture diameter from 300 to 60 μm, corresponding to from 2.10 to 0.42 Airy unit, which represents the theoretically derived Airy disk diameter. Magnification view of the cell periphery also clearly visualized structures of filopodia that are in tight contact with the hydrogel surface. These results clearly indicate that the interferometric microscopy developed here enables one to visualize the adhesion zone of cells adherent to 6–7 μm thick hydrogels, which is not possible by conventional RICM.

In the final step, we applied the interferometric microscopy to evaluate the impact of substrate elasticity on the adhesion of B16-F10 cells. Cells were cultured for 3 h on PAAm gels with E = 9.8, 13.2, and 62.5 kPa and then fixed. Bright field microscopy images (Figure 4a) imply that B16-F10 exhibited a more pronounced spreading on stiffer gels, and the zones of cell-hydrogel tight contacts are identified as black patches in interferometric images (Figure 4b). Such black area is also found for B16-F10 cells on hard glass substrate coated with fibronectin (Figure S1, Supporting Information), which renders the specific binding to its receptor proteins such as integrin. To define cell-hydrogel tight contacts, we first draw lines along the cell contour (Figure S2, Supporting Information). Then minimum intensity within the contour was taken as I_{min}. I_{max} was carefully determined from interference fringes originated from cell bottom membranes and hydrogels at cell periphery (see Figure S3 and Supporting Information). Finally, we clip the adhesion zone from the interference images by intensity threshold of 20% with the equation, $I \leq 0.2 \times (I_{max} - I_{min}) + I_{min}$. The clipped images (Figure 4c) clearly show patch-like adhesion structures, which were typically seen in RICM images of cells adhered to flat substrate.[6,9,18,19] The estimated total adhesion area is monotonically increased from 74 μm^2 578 μm^2 according to the increase in the stiffness of hydrogel from 9.8 ± 0.4 kPa to 62.5 ± 4.7 kPa, indicating mechano-response of B16-F10 cells.

These results clearly indicate our interferometric microscopy has the great potential to improve the contrast of cell-hydrogel contacts. The threshold level of 20% corresponds to the cell-hydrogel separation distance of ~40 nm according to eq 1. However, the reconstruction of absolute distance between cells and substrate from images of monochromatic RICM is generally challenging, because I_{min} and refractive index remains unclear.[20−23] Nevertheless, such ambiguities can be eliminated by determining optical phase with two different wavelengths in dual wave RICM.[24−26] In fact, the two different periodicities of fringe patterns by a diode laser and SLD (Figure 2d) indicate the potential to combine the dual- (or multi-) wave RICM with our interferometry. Also, in the case of hydrogels, one should consider that the hydrogel–liquid interface is diffusive and therefore not defined as a sharp boundary like glass/liquid interfaces. In fact, X-ray and neutron reflectivity curves of highly swollen polymer layers at the solid/liquid interface can be fitted either by using a parabolic function[27,28] or by introducing several consecutive incremental steps.[29] Although PAAm gel/water interfaces are difficult to quantify by X-ray and neutron reflectivity due to low electron and neutron density contrast, X-ray reflectivity at high relative humidity revealed that the air/PAAm interface (PAAm film thickness ~ 100 nm) broaden in the range of several nanometers,[30] which may be a potential resolution to determine the thickness of hydrogel–solution interfaces.

In summary, we have succeeded in enhancing the contrast in interferometric patterns from cell–hydrogel contact zones by using a new class of RICM system combined with (i) a confocal unit, (ii) high throughput optics, and (iii) coherent monochromatic light sources. We successfully visualized physical contacts between cells and hydrogels, which allows

dx.doi.org/10.1021/jz402463u | J. Phys. Chem. Lett. 2014, 5, 253−257

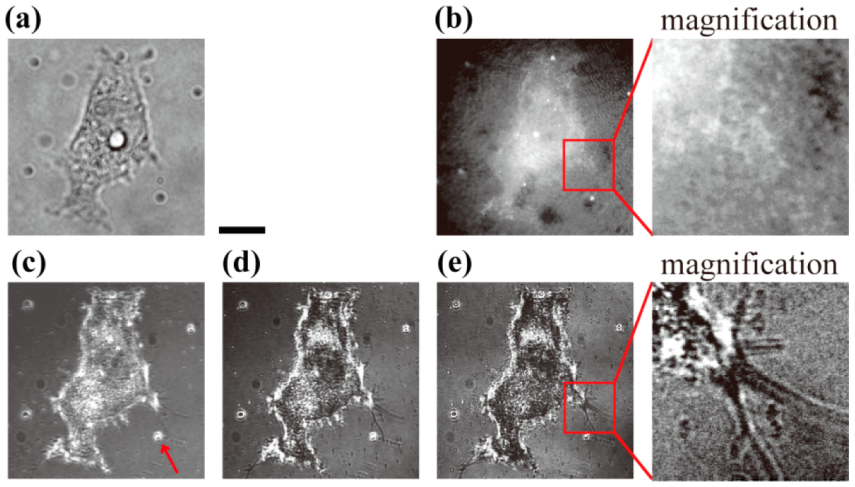

Figure 3. A B16-F10 cell on a PA gel (E = 13.2 ± 0.5 kPa) measured by (a) bright field microscopy, (b) conventional RICM, and (c–e) advanced interferometric microscopy. Diameter of confocal apertures is (c) 300 μm, (d) 150 μm, and (e) 60 μm. SLD (λ = 680 nm) was used as a light source for the advanced interferometric microscopy. Images at the right of panels b and e are magnification of cell periphery. Scale bars: 10 μm. The bright dots like the one indicated by a red arrow in panel c are polystyrene beads embedded in PAAm gels.

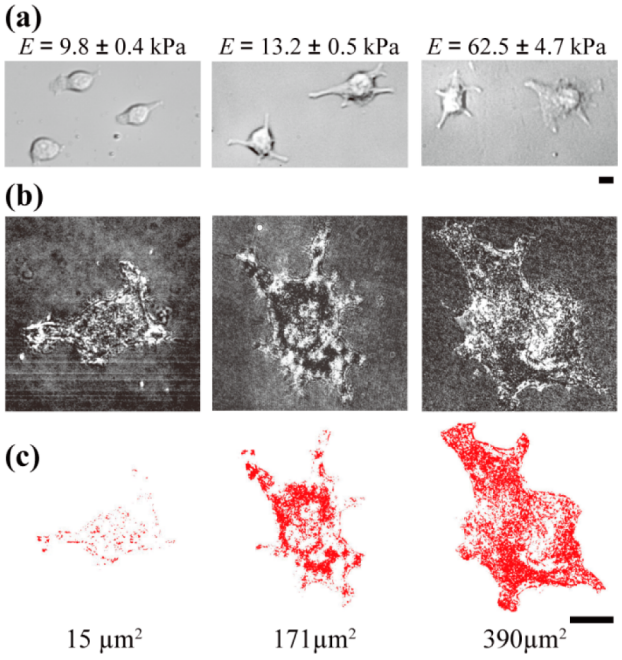

Figure 4. B16-F10 cells on PAAm gels with three different stiffness (E = 9.8 ± 0.4 kPa, E = 13.2 ± 0.5 kPa, E = 62.5 ± 4.7 kPa) were measured by (a) bright field microscopy and (b) interferometric microscopy developed in this study. Laser (λ = 532 nm) was utilized as a light source. (c) Clipped contact area according to eq 1. Diameter of a confocal aperture was 60 μm. Scale bars: 10 μm.

for the determination of areas of cell-hydrogel adhesion. We foresee that our advanced interferometric optical microscopy will provide quantitative insights into cell adhesion to various hydrogels, which contribute to the understanding of mechanical interactions between cells and soft substrates.

■ ASSOCIATED CONTENT

Ⓢ Supporting Information

An interferometric image of a cell on glass substrate, the method of determining the calculating area, and maximum intensity "I_{max}" are described. This material is available free of charge via the Internet at http://pubs.acs.org.

■ AUTHOR INFORMATION

Corresponding Author

*E-mail: hiroshi@mail.saitama-u.ac.jp; Tel/FAX: +8148-858-3814.

Notes

The authors declare no competing financial interest.

■ ACKNOWLEDGMENTS

The present work was supported by grants from the Japan Society for the Promotion of Science (JSPS) KAKENHI (Nos. 24680050, 24106505, and 24656006) and the Joint Research Program of the Institute of Low Temperature Science (Hokkaido University) to H.Y.Y. M.T. thanks the German Science Foundation (SFB 873) for the support. M.T. is a member of the German Excellence Cluster "CellNetwork" and the Helmholtz Program "BioInterface". The iCeMS is supported by the World Premier International Research Center Initiative (WPI), MEXT, Japan. T.M. acknowledges a Grant-in-Aid for JSPS fellows (No. 25 8820). We also thank Orpheus Chatzivasiliou for stimulating discussion about image analysis.

■ REFERENCES

(1) Discher, D. E.; Janmey, P.; Wang, Y. Tissue Cells Feel and Respond to the Stiffness of Their Substrate. *Science* **2005**, *310*, 1139–1143.

(2) Engler, J. A.; Sen, S.; Sweeney, H. L.; Discher, D. E. Matrix Elasticity Directs Stem Cell Lineage Specification. *Cell* **2006**, *126*, 677–689.

(3) Funatsu, T.; Harada, Y.; Tokunaga, M.; Saito, K.; Yanagida, T. Imaging of Single Fluorescent Molecules and Individual ATP Turnovers by Single Myosin Molecules in Aqueous Solution. *Nature* **1995**, *374*, 555–559.

(4) Curtis, A. S. G. The Mechanism of Adhesion of Cells to Glass. A Study by Interference Reflection Microscopy. *J. Cell Boil.* **1964**, *20*, 199–215.

(5) Ploem, S. J. Reflection-Contrast Microscopy as a Tool for Investigation of the Attachment of Living Cells to a Glass Surface; Blackwell: Oxford, 1975.

(6) Izzard, C. S; Lochner, L. R. Cell-to-Substrate Contacts in Living Fibroblasts: An Interference Reflection Study with an Evaluation of the Technique. *J. Cell. Sci.* **1976**, *21*, 129−159.
(7) Gingell, D.; Todd, I. Interference Reflection Microscopy. A Quantitative Theory for Image Interpretation and Its Application to Cell-Substratum Separation Measurement. *Biophys. J.* **1979**, *26*, 507−526.
(8) Rädler, J.; Sackmann, E. Imaging Optical thickness and Separation Distances of Phospholipid Vesicles at Solid Surfaces. *J. Phys. II France* **1993**, *3*, 727−748.
(9) Limozin, L.; Sengupta, K. Quantitative Reflection Interference Contrast Microscopy (RICM) in Soft Matter and Cell Adhesion. *ChemPhysChem* **2009**, *10*, 2752−2768.
(10) Cai, N.; Wong, C. C.; Gong, Y. X.; Tan, S. C. W.; Chan, V.; Liao, K. Modulating Cell Adhesion Dynamics on Carbon Nanotube Monolayer Engineered with Extracellular Matrix Proteins. *Appl. Mater. Inter.* **2010**, *2*, 1038−1047.
(11) Li, X.; Feng, H.; Chen, W. N.; Chan, V. Hepatitis B Virus Induced Coupling of Deadhesion and Migration of HepG2 Cells on Thermo-Responsive Polymer. *Biomaterials* **2010**, *31*, 1894−1903.
(12) Wen, R.; Lahiri, A.; Azhagurajan, M.; Kobayashi, S.; Itaya, K. A New in Situ Optical Microscope with Single Atomic Layer Resolution for Observation of Electrochemical Dissolution of Au(111). *J. Am. Chem. Soc.* **2010**, *132*, 13657−13659.
(13) Sazaki, G.; Matsui, T.; Tsukamoto, K.; Usami, N.; Ujihara, T.; Fujiwara, K.; Nakajima, K. In Situ Observation of Elementary Growth Steps on the Surface of Protein Crystals by Laser Confocal Microscopy. *J. Cryst. Growth* **2004**, *262*, 536−542.
(14) Suzuki, Y.; Sazaki, G.; Matsumoto, M.; Nagasawa, M.; Nakajima, K.; Tamura, K. First Direct Observation of Elementary Steps on the Surfaces of Glucose Isomerase Crystals under High Pressure. *J. Cryst. Growth* **2009**, *9*, 4289−4295.
(15) Sazaki, G.; Zepeda, S.; Nakatsubo, S.; Yokoyama, E.; Furukawa, Y. Elementary Steps at the Surface of Ice Crystals Visualized by Advanced Optical Microscopy. *Proc. Natl. Acad. Sci. U. S. A.* **2010**, *107*, 19702−19707.
(16) Tse, J. R.; Engler, A. J. Preparation of Hydrogel Substrates with Tunable Mechanical Properties. In *Current Protocols in Cell Biology*; John Wiley & Sons: New York, 2010; pp 1−16.
(17) Buxboim, A.; Rajagopal, K.; Brown, A. E. X.; Discher, D. E. How Deeply Cells Feel: Methods for Thin Gels. *J. Phys.: Condens. Matter* **2010**, *22*, 194116.
(18) He, T.; Shi, Z. L.; Fang, N.; Neoh, K. G.; Kang, E. T.; Chan, V. The Effect of Adhesive Ligands on Bacterial and Fibroblast Adhesions to Surfaces. *Biomaterials* **2009**, *30*, 317−326.
(19) Modulevsky, D. J; Tremblay, D.; Gullekson, C.; Bukoresthliev, N. V.; Pelling, A. E. The Physical Interaction of Myoblasts with the Microenvironment during Remodeling of the Cytoarchitecture. *PLoS ONE* **2012**, *7*, e45329.
(20) Sackmann, E.; Bruinsma, R. F. Cell Adhesion as Wetting Transition? *ChemPhysChem* **2002**, *3*, 262−269.
(21) Bereiter-Hahn, J.; Fox, C. H.; Thorell, B. Quantitative Reflection Contrast Microscopy of Living Cells. *J. Cell Biol.* **1979**, *82*, 767−779.
(22) Braun, D.; Fromherz, P. Fluorescence Interferometry of Neuronal Cell Adhesion on Microstructured Silicone. *Phys. Rev. Lett.* **1998**, *81*, 5241−5244.
(23) Limozin, L.; Sengupta, K. Modulation of Vesicle Adhesion and Spreading Kinetics by Hyaluronan Cushions. *Biophys. J.* **2007**, *93*, 3300−3313.
(24) Sengupta, K.; Schilling, J.; Marx., S.; Fishcer, M.; Bacher, A.; Sackmann, E. Mimicking Tissue Surface by Supported Membrane Coupled Ultrathin Layer of Hyaluronic Acid. *Langumuir* **2003**, *19*, 1775−1781.
(25) Schilling, J.; Sengupta, K.; Goennewein, S.; Bausch, A. R.; Sackmann, E. Absolute Interfacial Distance Measurements by Dual-Wavelength Reflection Interference Contrast Microscopy. *Phys. Rev. E.* **2004**, *69*, 021901.
(26) Mundinger, T. A.; Sommerfeld, A.; Reinehr, R.; Spatz, J. P.; Häussinger, D.; Boehm, H. Investingating Cell-ECM Contact Changes in Response to Hypoosmotic Stimulation of Hepatocytes In Vivo with DW-RICM. *Plos ONE* **2012**, *7*, e48100.
(27) Milner, S. T.; Witten, T. A.; Cates, M. E. Theory of the Grafted Polymer Brush. *Macromolecules* **1988**, *21*, 2610−2619.
(28) Kuhl, T. L.; Majewski, J.; Wong, J. Y.; Steinberg, S.; Leckband, D. E.; Israelachvili, J. N.; Smith, G. S. A neutron Reflectivity Study of Polymer-Modified Phospholipid Monolayers at the Solid-Solution Interface: Polyethylene Glycol-Lipids on Silane-Modified Substrates. *Biophys. J.* **1998**, *75*, 2352−2362.
(29) Wong, J. Y.; Majewski, J.; Seitz, M.; Park, C. K.; Israelachvili, J. N.; Smith, G. S.; Polymer-Cushioned Bilayers, I. A Structural Study of Various Preparation Methods Using Neutron Reflectometry. *Biophys. J.* **1999**, *77*, 1445−1457.
(30) Mukherjee, M.; Singh, A.; Daillant, J.; Menelle, A.; Cousin, F. Effect of Solvent−Polymer Interaction in Swelling Dynamics of Ultrathin Polyacrylamide Films: A Neutron and X-ray Reflectivity Study. *Macromolecules* **2007**, *40*, 1073−1080.